Photoluminescence dynamics in few-layer InSe

Supplemental material

Tommaso Venanzi[1,2], Himani Arora[1,2], Stephan Winnerl[1], Alexej Pashkin[1], Phanish Chava[1,2], Amalia Patanè[3], Zakhar D. Kovalyuk[4], Zakhar R. Kudrynskyi[3], Kenji Watanabe[5], Takashi Taniguchi[5], Artur Erbe[1], Manfred Helm[1,2], and Harald Schneider[1]

1 Helmholtz-Zentrum Dresden-Rossendorf, 01314 Dresden, Germany

2 Technische Universität Dresden, 01062 Dresden, Germany

3 School of Physics and Astronomy,

University of Nottingham, Nottingham NG7 2RD, UK

4 Institute for Problems of Materials Science,

The National Academy of Sciences of Ukraine, Chernivtsi, Ukraine and

5 National Institute for Material Science,

1-1 Namiki, Tsukuba, 305-0044, Japan

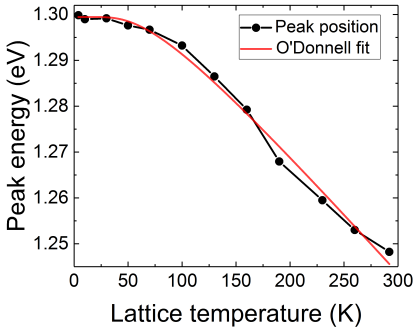

FIG. 1: Energy bandgap of InSe obtained from the model discussed in the main text (equation (1)) with respect to lattice temperature. The fit curve in red has been produced with the O'Donnell model.

I. O'DONNELL MODEL AND RAMAN SPECTRUM

Figure 1 shows the temperature dependence of the energy bandgap for the direct-bandgap sample (24-layer). We observe a typical redshift with temperature of the PL emission as consequence of the decrease of the bandgap energy due to the lattice expansion and to the interaction with phonons. The semi-empirical O'Donnell model ($E_g(T) = E_0 - S\,\hbar\omega(\coth(\frac{\hbar\omega}{kT}) - 1)$) [1] can reproduce the dependence of the peak energy position E_g on temperature with good accuracy. From the fitting, $E_0 = 1.299$ eV is the PL energy at zero Kelvin, $S = 1.55$ is a dimensionless coupling constant, and $\hbar\omega = 18 \pm 1$ meV $= 145 \pm 8$ cm^{-1} is an average phonon energy. We note that the average phonon energy obtained by this fit is close to the values of the energy of the optical phonons as measured by Raman (see Figure 2) and FTIR spectroscopy[2–4].

In figure 2, a Raman spectrum of the 24-layer InSe sample is shown. We observed three phonons at 115 cm^{-1}, 177 cm^{-1} and 227 cm^{-1} in good agreement with literature [2]. The observed peaks are slightly redshifted with respect to literature values of sample with the same thickness. This fact could be due to a slight strain in the flake [5].

II. MODEL FOR THE PL LINESHAPE

The PL intensity is given by the following expression according to Katahara model [6]:

$$I_{PL}(E) \propto \frac{E^2 a(E)}{\exp(\frac{E-\Delta\mu}{kT_{PL}}) - 1} \cdot \left(1 - \frac{2}{\exp(\frac{E-\Delta\mu}{2kT_{PL}}) + 1}\right) \tag{1}$$

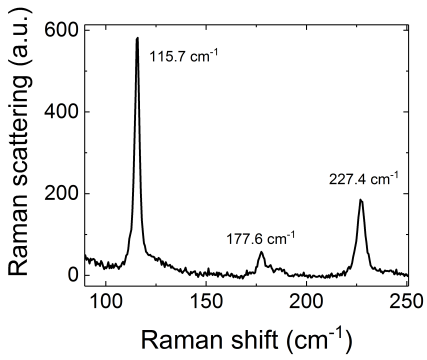

FIG. 2: Raman spectrum of thin-layer InSe. The excitation wavelength is 532 nm. The thickness of the flake is 20 nm.

where the first part is the connection between Planck's law and the absorption, and the second part in bracket is a small correction that takes into account the occupation of the bands (Pauli blocking). Here, $a(E)$ is the absorption, $\Delta\mu$ is the quasi-Fermi energy, and T_{PL} is the effective photoluminescence temperature. We note that in many cases the part of the expression containing the temperature can be simplified assuming a Boltzmann distribution. The quasi-Fermi energy is an effective Fermi energy for conduction and valence bands.

In order to fit the data, we need to get an expression for the absorption. We assume an exponential decay distribution as sub-bandgap density of states $\sim E_u \exp(-\frac{E}{E_u})\theta(E)$, where E_u is the Urbach energy. After convolution with a 3-dimensional density of states (DOS) $D(E) \propto \sqrt{E - E_g}$, where E_g is the bandgap energy, the absorptivity is:

$$\alpha_B(E) \propto E_u^{\frac{5}{2}} \begin{cases} e^{\frac{E-E_g}{E_u}} & : E < E_g \\ \sqrt{\frac{4(E-E_g)}{\pi E_u}} + \mathrm{erfc}(\sqrt{\frac{E-E_g}{E_u}})e^{\frac{E-E_g}{E_u}} & : E \geq E_g \end{cases} \tag{2}$$

where erfc() is the complementary error function. For energy below the bandgap, the function is an exponential rise (Urbach) and above it is the usual 3D DOS. The last term assures that the function belongs to the class of C_1 functions (the function is differentiable). To get a visual understanding of the model, we show the different components of absorption and PL in figure 3.

We have assumed an exponential sub-bandgap tail because of the clear mono-exponential decay of the low-energy side of the PL peak as shown in figure 4a.

In order to take into account the excitonic absorption, we add a Gaussian peak to the total absorption:

$$\alpha_X(E) \propto \frac{1}{\sqrt{\pi\sigma^2}} e^{-(\frac{E-E_X}{\sigma})^2} \tag{3}$$

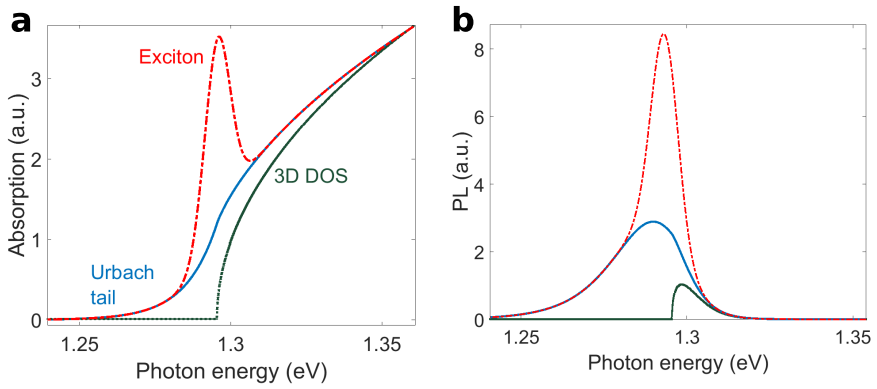

FIG. 3: (a) Absorption related to the 3 dimensional DOS, Urbach tail and exciton. (b) PL obtained considering the thermal occupation of the states shown in absorption.

where E_X is the exciton energy, and σ is the broadening of the exciton resonance. Therefore we get $\alpha(E) = \alpha_B(E) + p\ \alpha_X(E)$ where p is the relative weight of the exciton absorption. With this parameter we can extrapolate the exciton contribution.

Considering also the small thickness of our sample, we assumed a linear relation between absorption and absorptivity $a(E) = \alpha(E)d$ where d is the thickness of the sample. So finally we can plug $a(E)$ into equation 1.

The fitting function can reproduce the PL data for each temperature with excellent accuracy as shown for example in figure 4 for $T = 4$ K and $T = 160$ K. In particular in figure 4a the fit obtained without the exciton contribution is shown. Furthermore in figure 4c the free electron-hole and exciton contributions are shown separately.

III. PL TEMPERATURE AT ZERO KELVIN T_0

The PL temperature at zero Kelvin T_0 is mostly due to the inhomogeneous broadening of the PL band. In real system, the PL band does not reach the limit of homogeneous broadening even at $T_{Lattice} = 0$ K. Therefore, T_0 can be used as a measure for the disorder potential in the material.

Figure 5a shows the dependence of the parameter T_0 on the number of layers. T_0 was obtained for each sample by fitting the PL line at $T_{Lattice} = 4$ using the model presented in the main text. Then, $T_0 = \sqrt{T_{PL}^2 - T_{Lattice}^2}$. T_0 increases upon decreasing the number of layers. This indicates that the disorder potential is more pronounced for thinner samples.

In figure 5b, the dependence of the effective PL temperature T_0 on excitation power is

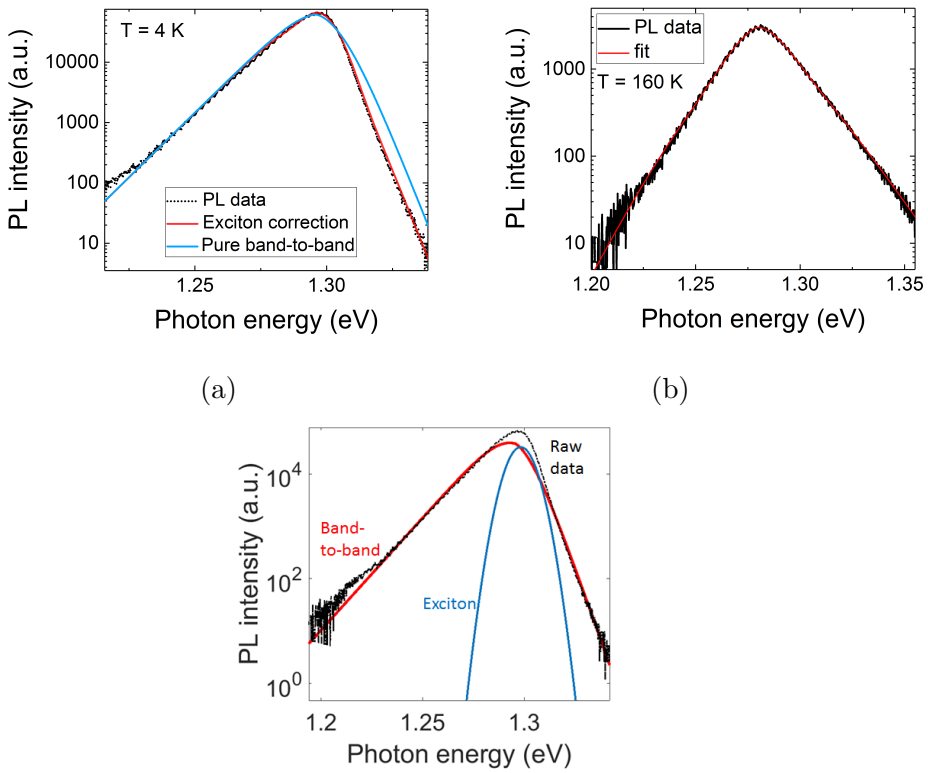

FIG. 4: (a) and (b) PL emission at 4 K and 160 K with fit as described in the text. (c) Free electron-hole and exciton contribution as obtained by the model described above.

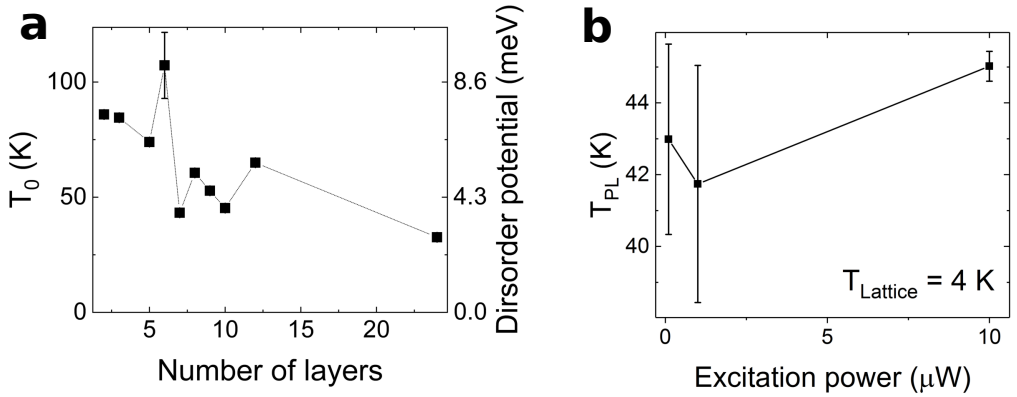

FIG. 5: (a) Dependence of the effective PL temperature at zero Kelvin T_0 on the number of layers. T_0 increases upon decreasing the number of layers, indicating higher disorder potential for thinner samples. (b) Dependence of the effective PL temperature on excitation power at $T_{Lattice} = 4$ K.

shown. We observed only a slight contribution from the excitation power. Therefore the PL temperature is related to an inhomogeneous broadening of the PL line rather than carrier heating due to the photo-excitation.

IV. DECOMPOSITION OF THE PL DECAY

Figure 6a shows the PL emission as a function of time and photon energy of a 24-layer InSe crystal. First we integrated the PL data with respect to the photon energy and then we fitted the PL decay with a bi-exponential function.

After that, we fixed the time constants ($\tau_1 = 7.7 \pm 0.2$ ns and $\tau_2 = 49 \pm 6$ ns in the case shown in figure 6) and we fitted the PL decay with bi-exponential function at each photon energy. Figure 6b shows the obtained fit of the PL data. Figures 6c and 6d show the decomposed fast and slow component of the PL decay.

The two components are spectrally separated now. In the main text the spectra of each component is shown.

We further note that the same procedure was applied to samples with other thicknesses with similar results.

[1] K. P. O'Donnell and X. Chen, Applied Physics Letters **58**, 2924 (1991).

[2] S. Lei, L. Ge, S. Najmaei, A. George, R. Kappera, J. Lou, M. Chhowalla, H. Yamaguchi, G. Gupta, R. Vajtai, A. D. Mohite, and P. M. Ajayan, ACS Nano **8**, 1263 (2014).

[3] O. Del Pozo-Zamudio, S. Schwarz, J. Klein, R. C. Schofield, E. A. Chekhovich, O. Ceylan, E. Margapoti, A. I. Dmitriev, G. V. Lashkarev, D. N. Borisenko, N. N. Kolesnikov, J. J. Finley, and A. I. Tartakovskii, ArXiv **1506-05619**, 1 (2015).

[4] N. M. Gasanly, V. Yavadov, B.M. andTagirov, and E. Vinogradov, Physica status solidi **43**, 5 (1978).

[5] Y. Li, T. Wang, M. Wu, T. Cao, Y. Chen, and R. Sankar, 2D Materials **5**, 021002 (2018).

[6] J. K. Katahara and H. W. Hillhouse, Journal of Applied Physics **116**, 173504 (2014).

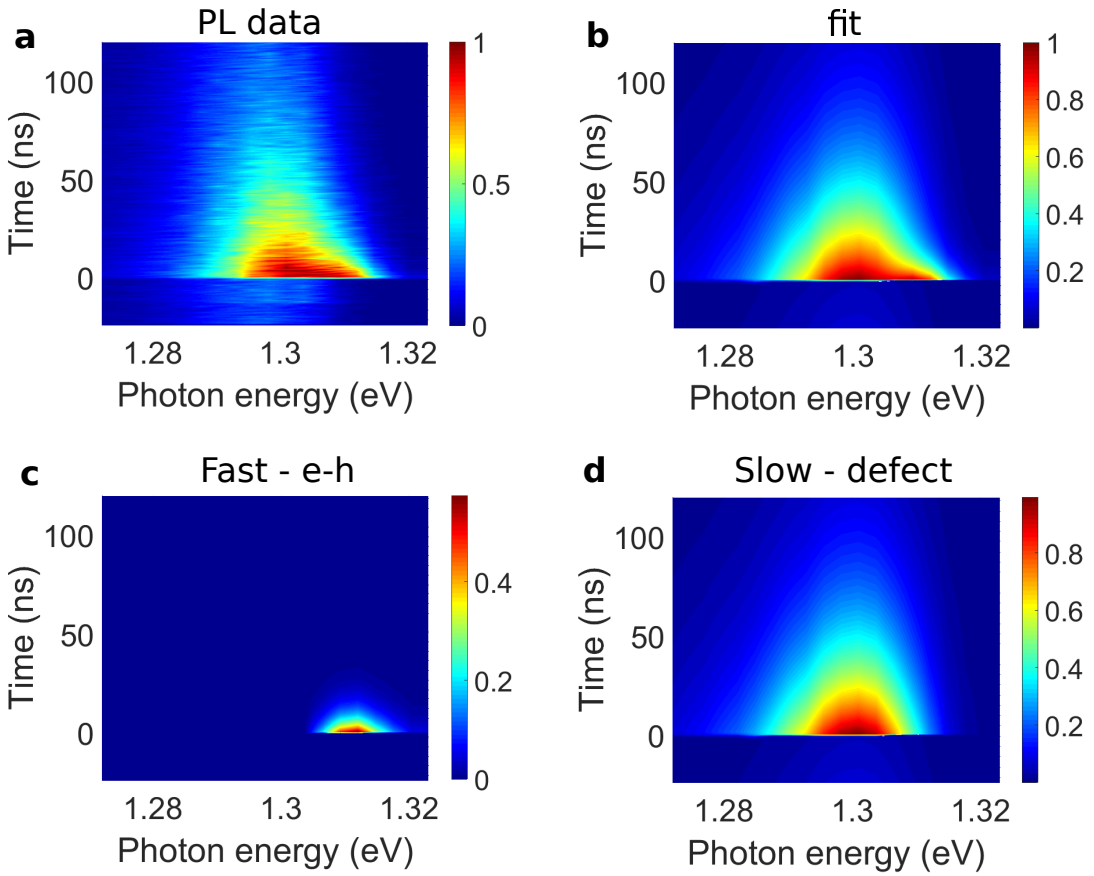

FIG. 6: (a) Normalized PL of a 24-layer thick sample as a function of time and photon energy. (b) Bi-exponential fit of the PL at each photon energy. The decay constants were kept fixed for each photon energy ($\tau_1 = 7.7 \pm 0.2$ ns and $\tau_2 = 49 \pm 6$ ns (c) and (d) Fast and slow components of the PL emission as extracted from the fit.